

Infrared outbursts as potential tracers of common-envelope events in high-mass X-ray binary formation

Lidia M. Oskinova^{1,4}, Tomasz Bulik^{2,4}, Ada Nebot Gómez-Morán³

¹Institute for physics and astronomy, University of Potsdam, Karl-Liebknecht-Str. 24/25, D-14476 Potsdam, Germany
e-mail: lida@astro.physik.uni-potsdam.de

²Astronomical Observatory, University of Warsaw, Aleje Ujazdowskie 4, 00478 Warsaw, Poland

³Université de Strasbourg, CNRS, Observatoire astronomique de Strasbourg, UMR 7550, F-67000 Strasbourg, France

⁴Kavli Institute for Theoretical Physics, University of California, Santa Barbara, CA 93106, USA

March 2, 2022

ABSTRACT

Context. Classic massive binary evolutionary scenarios predict that a transitional common-envelope (CE) phase could be preceded as well as succeeded by the evolutionary stage when a binary consists of a compact object and a massive star, that is, a high-mass X-ray binary (HMXB). The observational manifestations of common envelope are poorly constrained. We speculate that its ejection might be observed in some cases as a transient event at mid-infrared (IR) wavelengths.

Aims. We estimate the expected numbers of CE ejection events and HMXBs per star formation unit rate, and compare these theoretical estimates with observations.

Methods. We compiled a list of 85 mid-IR transients of uncertain nature detected by the Spitzer Infrared Intensive Transients Survey and searched for their associations with X-ray, optical, and UV sources.

Results. Confirming our theoretical estimates, we find that only one potential HMXB may plausibly associated with an IR-transient and tentatively propose that X-ray source NGC 4490-X40 could be a precursor to the SPIRITS 16az event. Among other interesting sources, we suggest that the supernova remnant candidate [BWL2012] 063 might be associated with SPIRITS 16ajc. We also find that two SPIRITS events are likely associated with novae, and seven have potential optical counterparts.

Conclusions. The massive binary evolutionary scenarios that involve CE events do not contradict currently available observations of IR transients and HMXBs in star-forming galaxies.

Key words. Stars: Massive

1. Introduction

Massive stars are born and evolve in binaries, often as part of a higher-order hierarchical system (e.g., Paczyński 1971; Vanbeveren et al. 1998). The binary components can expel and exchange mass, can merge, or become unbound. Stellar and binary evolution are strongly affected by these processes. Among a large variety of possible evolutionary scenarios, we can distinguish three key stages. In the first stage, both components are non-degenerate stars, while in the next evolutionary stage, one of the binary components collapses to become a neutron star (NS) or a black hole (BH). The accretion of matter lost by the remaining non-degenerate star onto an NS or BH can power strong X-ray emission. Such systems are usually observed as high-mass X-ray binaries (HMXBs). In the final evolutionary stage, both binary components are degenerate and form a relativistic binary (Postnov & Yungelson 2014, and references therein).

While the physics of binaries in each evolutionary stage is intensively studied and is reasonably well established, the transitions between evolutionary stages are still poorly understood. Among the major uncertainties in massive binary evolution is a transitional phase during which binary components are embedded in a shared or common envelope (CE) (Paczynski 1976). Such a phase occurs when a much more massive star fills its Roche lobe and starts to transfer mass onto the less massive companion. The orbit shrinks and the mass transfer is unstable. Dur-

ing this phase, the friction between the stars and the surrounding envelope moves the stars closer to each other. The resulting surplus of the orbital energy is eventually spent to disperse the CE and eject its material into the interstellar medium (ISM) (Iben & Livio 1993).

Although quantitative arguments on the CE physics are broadly discussed (see review by Ivanova et al. 2013), there is a dearth of quantitative studies capable to make exact predictions on the observable properties of CEs and their final ejections (MacLeod et al. 2017; Iaconi et al. 2017, and references therein). Recent studies have suggested that the CE phase in some binaries could end with the CE ejection, which might be observable as an IR transient (Blagorodnova et al. 2017).

The “standard scenario” of massive binary evolution from a main-sequence star to a relativistic binary (van den Heuvel & De Loore 1973; Tutukov & Yungelson 1973) predicts that the CE also occurs in the stage when the primary star has already become a compact object. The evolutionary chain of events runs through the stage of an HMXB powered by the matter accretion from the secondary star onto the compact object (see, e.g., Fig. 7 in Postnov & Yungelson 2014). When the secondary fills its Roche lobe, it engulfs the compact object, forming a CE. In this phase, the accretion of the CE material onto a BH is unavoidable, and the system should be visible as a strongly obscured X-ray source. The CE is eventually expelled, and the orbit shrinks by a factor of up to

a hundred. If a merger of the compact object and the secondary star's core is avoided, a binary is formed that consists of a He-star and a compact object on a close orbit. Such a binary is an HMXB that is powered by wind accretion. This scenario is a required ingredient in the formation of merging BHs similar to GW 150914 (see Fig. 1 in Belczynski et al. 2016).

There may be observational support for this scenario. Recently, a new class of obscured HMXBs was identified. In these systems, a large amount of circumstellar material effectively absorbs X-rays from an accreting compact object (Hynes et al. 2002; Fillard & Chaty 2004; Servillat et al. 2014; Lau et al. 2016, 2017). The donors in these objects are likely sgB[e] stars (Lamers et al. 1998). We may speculate that sgB[e] HMXBs roughly correspond to the systems where a compact object orbits a massive star core that is surrounded by a CE or its remnant material.

In this Letter we take a simple Ansatz that some IR transients are related to the ejection of the CE. We estimate the expected numbers of CE events and HMXBs in a star-forming galaxy and compare these estimates with observations by searching for possible X-ray counterparts to the IR transients.

The time is now well suited to investigate the associations between IR-transients and X-ray sources. Powerful X-ray observatories, *Chandra* and *XMM-Newton*, are operating since 2000. Although neither of these observatories has conducted an all-sky survey, their respective source catalogs are already very sizable. Since 2014, the *Spitzer* IR telescope conducts a systematic search for mid-IR transients in nearby galaxies, the *Spitzer* Infrared Intensive Transients Survey (SPIRITS) (see the survey overview in Kasliwal et al. 2017). The survey has identified a new type of events whose nature is not yet known. These events have infrared luminosities between novae and supernovae and occur in star-forming galaxies. Their unknown nature and association with star-forming regions opens a room for a suggestion that some of these events may be associated with a CE ejection. In this Letter we test this hypothesis.

In Section 2 we use basic binary evolution considerations to predict the number of CE events and HMXBs in a star-forming galaxy. Section 3 describes the work done to search for correlations between IR-transients and X-ray sources. The conclusions are presented in sect. 4. The notes on individual objects and the table summarizing our catalog searches are presented in the appendix.

2. Expected number of CE events

In order to estimate the number of CE events in a star-forming galaxy, we must consider the binary evolution leading to such phases. We choose a qualitative approach based on making physically plausible assumptions rather than a full population synthesis modeling. The key goal of this work is to check whether our basic understanding of massive binary evolution contradicts currently available observations of star-forming galaxies.

The initial state of the binary is determined by the mass of the primary M_{1i} , the mass ratio $q = M_{2i}/M_{1i}$, and the orbital separation A_i . We assume for simplicity that the initial orbits are circular.

We assume that the distribution of the primary mass is given by the initial mass function (IMF) $\zeta(M)$ (Kroupa et al. 1993) with the lowest stellar mass $M_{\min} = 0.08M_{\odot}$, and the maximum stellar mass $M_{\max} = 100M_{\odot}$. This assumption on the upper stellar mass is conservative. In very massive star clusters, the most massive stars could have masses of at least $150M_{\odot}$ (Figer 2005; Weidner & Kroupa 2006). Moreover, the IMF may depend on

metallicity becoming more top-heavy with decreasing metallicity (Marks et al. 2012); this suggestion is gaining observational support (Schneider et al. 2018; Ramachandran et al. 2018).

Furthermore, we assume that the distribution of mass ratios is $\Psi(q) \propto \text{const } k$ (Kobulnicky & Fryer 2007), and the distribution of the initial separations is $\Xi(A) \propto A^{-1}$, and we assume that the range of the orbital separations is $10R_{\odot} < A < 10^6R_{\odot}$. The range of the mass ratio takes into account the fact that the minimum mass of a star is $M_{\min} = 0.08M_{\odot}$, so that for a given mass of the primary M , we have $q_{\min}(M) = 0.08M_{\odot}/M$. We consider two cases for the evolution: the high and low initial mass ratio.

We first consider the case when the initial mass ratio is low, for instance, $q = q_{\text{div}}$, where $q_{\text{div}} \lesssim 0.25$ (for a discussion, see, e.g., Belczynski et al. 2008). As the primary evolves, it will fill the Roche lobe as long as the initial orbital separation is not too large, $A < 1000R_{\odot}$. Since the mass ratio is low, the mass transfer will be unstable and can be considered a CE event. As a result of the CE, the binary can merge if the initial orbital separation is small, $A < 100R_{\odot}$, otherwise it will survive. If it survives, the primary will be stripped of its envelope and may become a helium star, while the secondary will be essentially unchanged because it cannot accrete much matter in the short timescale of the CE event. The orbital separation will be greatly reduced (Webbink 1984). In this case, we do not expect an HMXB, neither preceding nor following the CE event.

In the case of a high mass ratio, where the masses are nearly equal, $q \gtrsim q_{\text{div}}$, the evolutionary scenario is different. The system enters into the first mass transfer that can be considered as non-conservative. It is initially unstable, and then stabilizes as the mass ratio is reversed. The orbit initially shrinks, but then expands, and the final orbital separation is close to the initial separation, $A_{\text{ps}} \approx A_i$ (Eggleton 2006). The system now consists of a core of the primary, possibly with some hydrogen envelope, and a rejuvenated secondary with an increased mass. The next stage of the evolution is due to the fast evolution of the core of the primary, which quickly explodes as a supernova, forming an NS or a BH. Formation of an NS is usually associated with a kick (Cordes & Chernoff 1998; Hobbs et al. 2005). As the system is still relatively wide, the kick can easily disrupt the system, and we assume that the survival probability of the system is $p_{\text{SN1}} \approx 0.1$.

Recent modeling has shown that the high Galactic latitudes of many black holes in low-mass X-ray binary systems could be explained only if these systems did obtain quite significant natal kicks, similar to those of NSs (Repetto et al. 2012). On the other hand, the gravitational wave observations constrain the kicks that BHs receive in high-mass mass binaries to about $\sim 50 - 200 \text{ km s}^{-1}$, that is, smaller than the NS kicks (Wysocki et al. 2018). The relatively small kicks imply a high survival probability of massive binaries after the primary collapse into a BH. Here, we assume for simplicity that the survival probability for BH systems is close to unity, $p_{\text{SN1}} \approx 1$ (see also Belczynski et al. 2008). In any case, as can be seen from Eq. (6), the predicted number of HMXBs is directly proportional to p_{SN1} and can therefore be easily corrected for lower values.

The supernova explosion affects the orbit size and introduces some ellipticity because of the mass loss and the kick. The system now consists of a compact object and a massive secondary, and it likely becomes an HMXB, as the massive secondary will have a strong stellar wind that will lead to accretion onto the compact object. The secondary star gradually increases its radius, fills the Roche lobe, and initializes rapid mass transfer onto the compact object. The mass transfer will now be unstable and can be described as a common envelope. If the orbital separation

is small, the compact object will plunge into the donor and form a Thorne-Zytkow object (Thorne & Zytkow 1975) or explode as a γ -ray burst (Fryer & Woosley 1998). We make a crude assumption that the system will survive the CE if the orbital separation is $A_{ps} \gtrsim 100 R_\odot$ (e.g., see Fig. 13 in Terman et al. (1995) and the discussion in Section 3.6 in Postnov & Yungelson (2014).)

We optimistically assume that the system survives the CE with the donor on the Hertzsprung gap (Dominik et al. 2012). Following the CE, the system will consist of a compact object in a tight binary with the core of the donor; most likely a helium star. The compact object will accrete matter either through the wind or through Roche-lobe overflow. Thus in this case, the CE event will also be followed by the formation of a new HMXB.

We calculate the rate of CE events in both scenarios. We assume that the star formation rate (SFR) is constant and denote the binary fraction as f_{bin} . The average mass of a single star is $\langle M \rangle_{sin} = \int M \zeta(M) dM$, and the average mass of a binary is $\langle M \rangle_{bin} = \int \int M(1+q) \zeta(M) \Psi(q) dM dq$. The average mass of a star in a population is then

$$M_{ave} = (1 + f_{bin})^{-1} ((1 - f_{bin}) \langle M \rangle_{sin} + f_{bin} \langle M \rangle_{bin}). \quad (1)$$

Assuming $f_{bin} = 0.5$, and $k = 0$, we obtain $M_{ave} = (5/6) \langle M \rangle_{sin} = 0.37 M_\odot$. The binary formation rate is $R_{bin} = \text{SFR} \times f_{bin} M_{ave}^{-1} = 1.35 (\text{SFR} / M_\odot \text{yr}^{-1}) \text{yr}^{-1}$.

In the first case, when $q < q_{div}$, the rate of the CE events can be obtained by integrating the relevant distributions:

$$N_{CE1} = R_{bin} f_A \int_{M_{min1}}^{M_{max}} \zeta(M) dM \int_{q_{min}(M)}^{q_{div}} \Psi(q) dq, \quad (2)$$

where M_{min1} is the lowest mass of the primary that we are interested in, $f_A = \int_{A_{min}}^{A_{max}} dA \Xi(A)$ is the fraction of systems with an initial orbital separation in the range between $A_{min} = 100 R_\odot$, and $A_{max} = 1000 R_\odot$. Given the above assumptions of the range for A , we obtain $f_A = 0.2$. The initial separations smaller than A_{min} will lead to a merger, while in the case of initial separations larger than A_{max} , the primary will not fill the Roche lobe. The value of M_{min1} can be obtained from the age of the population that is analyzed, as we consider only the stars that could have evolved within a given timescale. For a typical Milky Way-like galaxy, we use $M_{min1} = 1 M_\odot$.

In the second case, when $q > q_{div}$, the CE events rate is given by

$$N_{CE2} = R_{bin} P_{SN1} f_A \int_{M_{CO}}^{M_{max}} \zeta(M) dM \int_{q_{div}(M)}^1 \Psi(q) dq, \quad (3)$$

where $M_{CO} = 8 M_\odot$ is the minimum initial mass required to form a compact object: an NS, or a BH (Woosley et al. 2002). Incidentally, we can obtain the expected number of HMXBs that precede the CE phase in this case. To this end, we estimate the time that each binary is in the X-ray phase as roughly half of the lifetime of the secondary after rejuvenation. Given the short massive star lifetime, this crude assumption does not introduce large errors.

We assume that the mass of the secondary increases by half in the mass transfer and becomes $M_{2p} = 1.5 M_{1i} q$. The X-ray phase duration is then $T_X(M, q) = 0.5 T_\star(M_{2p}) \approx 5.7 \times 10^6 (10 M_\odot / (q M_{1i}))^{2.5}$ years, and the number of HMXBs is

$$N_{HMXB} = R_{bin} P_{SN1} f_A \int_{M_{min}}^{M_{max}} \zeta(M) dM \int_{q_{div}(M)}^1 \Psi(q) T_X(M, q) dq. \quad (4)$$

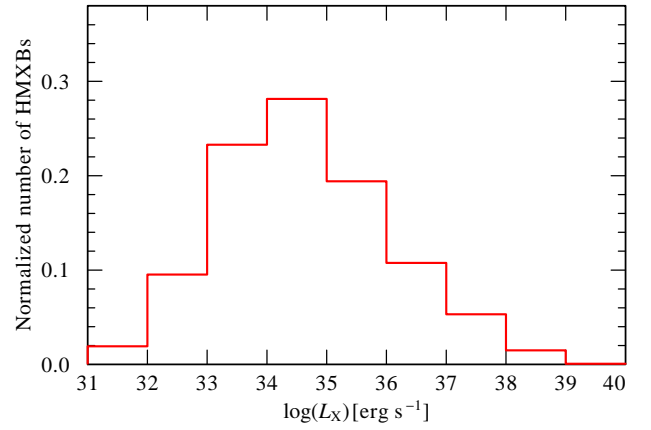


Fig. 1. Model X-ray luminosity probability distribution of wind-accreting HMXBs (see text for the model description).

We can also calculate the number of HMXBs per unit of star formation:

$$\frac{N_{HMXB}}{\text{SFR}} = \frac{f_{bin} P_{SN1} f_A}{M_{ave}} \int_{M_{min}}^{M_{max}} \zeta(M) dM \int_{q_{div}(M)}^1 \Psi(q) T_X(M, q) dq. \quad (5)$$

Inserting the numbers, we obtain

$$\frac{N_{HMXB}}{\text{SFR}} = 384 \frac{f_{bin}}{0.5} \frac{f_A}{0.2} \frac{P_{SN1}}{0.1} \text{yr} M_\odot^{-1}. \quad (6)$$

To roughly estimate the X-ray luminosity of HMXBs, we assumed that these systems are wind fed. We ran a set of 30 000 simulations on a grid of plausible stellar wind and binary parameters. Circular orbits with orbital separations in the range $2-20 R_*$ were assumed. Our model population consists of binaries with donor masses in the range $15-45 M_\odot$ and compact object masses in the range $1.4-14 M_\odot$ (the donor and compact object masses are not drawn from a mass function, but are located on a grid). For each donor star, we varied stellar wind parameters. Mass-loss rates in the range $\log \dot{M} = -7.5 \dots -5.5 [M_\odot \text{yr}^{-1}]$ are assigned to a donor of each mass. The rationale is that helium stars of relatively low present-day mass (such as Wolf-Rayet stars) could have prodigious mass-loss rates, while even quite massive stars could have low mass-loss rates at metallicities lower than solar (Bouret et al. 2003; Hainich et al. 2014; Shenar et al. 2016; Hainich et al. 2018). Terminal wind velocities in the range 500 km s^{-1} to 2500 km s^{-1} were adopted; at close binary separations ($< 5 R_*$), the wind velocity was roughly assumed to be a half of its terminal value (Sander et al. 2017). X-ray luminosities were calculated using the Bondi-Hoyle-Lyttleton approximation and accounting for relative velocities (using the same formalism as in Oskinova et al. 2012).

The histogram shown in Fig. 1 demonstrates that the X-ray luminosity of a wind-fed HMXB is likely to exceed $10^{34}-10^{35} \text{ erg s}^{-1}$, which is in good agreement with observations (Lutovinov et al. 2013). However, our model formalism neglects effects related to the neutron star spin and magnetic field (e.g., Illarionov & Sunyaev 1975; Bozzo et al. 2016) as well as the orbit eccentricity. These effects may lead to temporal arrest of accretion. It is known that the majority of observed HMXBs are transients (e.g. Walter et al. 2015; Martínez-Núñez et al. 2017). Taking this into account, the number of HMXBs estimated in Eq. (6) is in quite good agreement with empirically derived from the observations of X-ray sources in nearby galaxies (Mineo et al. 2011, 2012).

The SPIRITS survey has monitored 191 galaxies (Kasliwal et al. 2017). We do not have the estimate of the SFR for each of them, therefore we assume that they are similar to the Milky Way. The average SFR of the Milky Way varies in the literature from $5 M_{\odot} \text{yr}^{-1}$ to $0.7 M_{\odot} \text{yr}^{-1}$ (Smith et al. 1978; Misiriotis et al. 2006; Diehl et al. 2006; Murray & Rahman 2010; Robitaille & Whitney 2010). Adopting an SFR $3.6 M_{\odot} \text{yr}^{-1}$ per galaxy, the SPIRITS survey has examined a region with a total star formation rate of $\text{SFR} = 687 M_{\odot} \text{yr}^{-1}$. We now evaluate the expected rate of CE events in the low and high mass ratio case. Inserting the fiducial numbers in Eq. (2), we obtain

$$N_{\text{CE1}} = 3.0 \frac{f_{\text{bin}}}{0.5} \frac{\text{SFR}}{678 M_{\odot} \text{yr}^{-1}} \frac{f_{\text{A}}}{0.2} \text{yr}^{-1}, \quad (7)$$

for which we do not expect an X-ray source to precede or follow the CE. For the channel with a high mass ratio, where the CE events are associated with an X-ray source, we obtain from Eq. (3)

$$N_{\text{CE2}} = 0.03 \frac{f_{\text{b}}}{0.5} \frac{\text{SFR}}{678 M_{\odot} \text{yr}^{-1}} \frac{f_{\text{A}}}{0.2} \frac{p_{\text{SN1}}}{0.1} \text{yr}^{-1}. \quad (8)$$

Thus we expect that the SPIRITS survey sees only few events from the evolutionary channel with a low initial mass ratio, and there is a very small chance to observe a CE event associated with a HMXB.

3. Search for associations between mid-IR transients and X-ray sources

To compare these estimates with observations, we compiled a list of SPIRITS events reported in the Astronomer’s Telegrams (6644, 7929, 8688, 8940, 9434, 10171, 10172, and 10488) and in Kasliwal et al. (2017). The events of known nature are excluded from consideration, the remaining 85 IR events are listed in Table A.1. To search for X-ray sources that might be associated with SPIRITS events, as a first step, we conducted a blind search of X-ray catalogs allowing a generous cross-correlation radius. This search showed that the absolute majority of X-ray observations of galaxies hosting SPIRITS were made by the *Chandra* X-ray telescope. Hence, we decided to concentrate on the *Chandra* data as they provide positional accuracy compatible with that of the *Spitzer* IR telescope. In addition to searches in the catalogs of individual galaxies (when available), we also included the most recent meta-catalogs such as the “X-ray emission from star-forming galaxies - I. High-mass X-ray binaries” (Mineo et al. 2012), “The *Chandra* ACIS Survey of X-ray Point Sources in 383 Nearby Galaxies” (Liu 2011), and “The *Chandra* ACIS Survey of X-Ray Point Sources: The Source Catalog” (Wang et al. 2016).

We investigated the coverage of SPIRITS sources by X-ray observations. Of 85 SPIRITS IR-transients, only 7 were not in the field of view of *Chandra* or *XMM-Newton* observations. Using the *Chandra* science archive facility, we roughly estimated the total *Chandra* exposure time for each SPIRITS event (Table A.1). The exposure times are vastly different, and the upper limits for the potential X-ray counterparts of X-ray transients are not uniform. It is beyond the scope of this study to derive the upper limits on the X-ray non-detections, as we are mainly interested in finding positive matches.

As a next step, the cross-correlations between IR and X-ray sources were searched within a radius of $1''$. If an X-ray counterpart was suspected, the X-ray images and event lists

were retrieved and checked manually. This narrowed search returned an X-ray counterpart for only one object, SPIRITS 14ajc in the galaxy M 83 (Kasliwal et al. 2017). Relaxing the cross-correlation radius to $2''$ added X-ray sources that might be associated with SPIRITS 17mj in M 81 and SPIRITS 16az in the galaxy NGC 4490. These and other interesting objects are discussed in the appendix.

SPIRITS 16az is the best potential match we have found. It was discovered on 2016-3-5 in the galaxy NGC 4490. SPIRITS 16az has a likely optical counterpart, XMMOM J123027.7+413943, at $0''.7$ distance with a positional error of $0''.6$. The optical source was detected in 2004. No X-ray source is seen in early ~ 20 ks *Chandra* observations taken on 2000-11-03. In 2004, two *Chandra* observations were obtained about four months apart. On 2004-07-29, no X-ray source in the vicinity of 16az is seen (see left panel in Fig. A.1). On the other hand, on 2004-11-20, an X-ray source is detected about $1''$ away from 16az. This is significant, since both *Chandra* observations had similar exposure times of ~ 40 ks. The X-ray source seen on 2004-11-20, NGC 4490-X40, is listed in the *Chandra* catalogs by Mineo et al. (2012); Liu (2011) and Wang et al. (2016). With a $1''$ positional error on the X-ray source, the association between NGC 4490-X40 and 16az is plausible. The X-ray luminosity of NGC 4490-X40, $L_{\text{X}} \approx 4 \times 10^{37} \text{ erg s}^{-1}$ at 7.8 Mpc, is compatible with its being an HMXB. Further studies of NGC 4490-X40 are needed to unambiguously conclude whether this source is an HMXB and whether SPIRITS 16az was a CE ejection event.

In Table A.1 we compile the results of our study. Although we were not successful and did not find an unambiguous association between X-ray sources and IR-transients, the estimates presented in section 2 show that the one possible X-ray counterpart to an IR-transient is in agreement with the expected rate of CE ejections linked to the HMXB evolution for a sample of surveyed galaxies.

4. Summary and conclusions

Motivated by massive binary evolutionary scenarios that predict links between HMXBs and short CE events, we searched for X-ray counterparts of IR-transients. This was done by correlating the positions of 85 not yet identified transients observed by the *Spitzer* IR telescope with X-ray catalogs and images. We also checked available optical and UV catalogs to confirm an HMXB nature of any potential X-ray counterpart. We found potential pre-IR outburst optical counterparts, including H II regions, for seven SPIRITS events. While confirmations for these identifications are required, at least some IR-transients we consider here are probably linked to young massive stars. Two IR-transients in our sample of 85 objects are very plausibly associated with recent novae. We did not find an unambiguous HMXB counterpart to any of the IR-transients. Our best match is SPIRITS 16az, which might be linked with an optical source and an X-ray transient identified as the HMXB NGC 4490-X40. The relatively large positional error of the X-ray source prevents firm identification. Another interesting source is SPIRITS 16ajc, which is likely associated with a pre-outburst X-ray source, possibly the SNR candidate [BWL2012] 063.

From considerations of binary evolution, we estimated the expected numbers of CE events and HMXBs in star-forming galaxies. We conclude that

1) massive binary evolutionary scenarios predict that a CE stage can be immediately preceded and/or succeeded by an HMXB

stage. Assuming that a CE ejection could be observed as an IR outburst, in principle some IR-transients could have an X-ray counterpart prior to or post IR-outburst;

2) our estimates show that a few hundred HMXBs per one star formation rate unit could be expected in a galaxy. The good agreement between observed numbers of HMXBs in star-forming galaxies and these predictions provides a justification for our estimates of the expected CE events. Assuming that the visibility of CE ejection event is about one year, we estimate that there is $\sim 3\%$ chance to observe an associated IR transient in a sample of 191 galaxies observed in the SPIRITS survey, if each of these galaxies has an SFR similar to that of the Milky Way. Hence the expected rate of IR transients associated with CE ejection is $\approx 1.6 \times 10^{-4} \text{ yr}^{-1}$ per Milky Way-type galaxy;

3) the current lack of positive detections of a CE event associated with a massive X-ray binary does not contradict standard massive binary evolutionary scenarios.

Acknowledgements. The authors thank the referee for their very useful comments. This work has been financially supported by the Programme National Hautes Energies (PNHE), project 994584. LO and AN thank *Integrated Activities in the High Energy Astrophysics Domain* project for support that enabled this work. L.O. acknowledges support from the DLR grant 50 OR 1612. TB was supported by the FNP grant TEAM/2016-3/19. LO and TB thank Kavli Institute for Theoretical Physics, University of California, where this project have been initiated, for their support. This research has made use of the SIMBAD database, the VizieR catalogue access tool, operated at CDS, Strasbourg, France, and the High Energy Astrophysics Science Archive Research Center (HEASARC), which is a service of the Astrophysics Science Division at NASA/GSFC and the High Energy Astrophysics Division of the Smithsonian Astrophysical Observatory. The scientific results reported in this article are based to a significant degree on the data obtained from the Chandra and *XMM-Newton* Data Archives.

References

- Belczynski, K., Holz, D. E., Bulik, T., & O’Shaughnessy, R. 2016, *Nature*, 534, 512
- Belczynski, K., Kalogera, V., Rasio, F. A., et al. 2008, *ApJS*, 174, 223
- Blagorodnova, N., Kotak, R., Polshaw, J., et al. 2017, *ApJ*, 834, 107
- Blair, W. P., Winkler, P. F., & Long, K. S. 2012, *ApJS*, 203, 8
- Bouret, J.-C., Lanz, T., Hillier, D. J., et al. 2003, *ApJ*, 595, 1182
- Bozzo, E., Oskinova, L., Feldmeier, A., & Falanga, M. 2016, *A&A*, 589, A102
- Cordes, J. M. & Chernoff, D. F. 1998, *ApJ*, 505, 315
- Diehl, R., Halloin, H., Kretschmer, K., et al. 2006, *Nature*, 439, 45
- Dominik, M., Belczynski, K., Fryer, C., et al. 2012, *ApJ*, 759, 52
- Eggleton, P. 2006, *Evolutionary Processes in Binary and Multiple Stars*
- Figer, D. F. 2005, *Nature*, 434, 192
- Fillard, P. & Chaty, S. 2004, *ApJ*, 616, 469
- Fryer, C. L. & Woosley, S. E. 1998, *ApJ*, 502, L9
- Hainich, R., Oskinova, L. M., Shenar, T., et al. 2018, *A&A*, 609, A94
- Hainich, R., Rühling, U., Todt, H., et al. 2014, *A&A*, 565, A27
- Hobbs, G., Lorimer, D. R., Lyne, A. G., & Kramer, M. 2005, *MNRAS*, 360, 974
- Hornoch, K., Errmann, R., Sowicka, P., Humphries, N., & Vaduvescu, O. 2015, *The Astronomer’s Telegram*, 8180
- Hornoch, K. & Kucakova, H. 2014, *The Astronomer’s Telegram*, 6176
- Hynes, R. I., Clark, J. S., Barsukova, E. A., et al. 2002, *A&A*, 392, 991
- Iaconi, R., Reichardt, T., Staff, J., et al. 2017, *MNRAS*, 464, 4028
- Iben, Jr., I. & Livio, M. 1993, *PASP*, 105, 1373
- Illarionov, A. F. & Sunyaev, R. A. 1975, *A&A*, 39, 185
- Ivanova, N., Justham, S., Chen, X., et al. 2013, *A&A Rev.*, 21, 59
- Jencson, J. E., Kasliwal, M. M., Adams, S., et al. 2017, *The Astronomer’s Telegram*, 1017
- Jencson, J. E., Kasliwal, M. M., Tinyanont, S., et al. 2016, *The Astronomer’s Telegram*, 8688
- Kasliwal, M. M., Bally, J., Masci, F., et al. 2017, *ApJ*, 839, 88
- Kobulnicky, H. A. & Fryer, C. L. 2007, *ApJ*, 670, 747
- Kroupa, P., Tout, C. A., & Gilmore, G. 1993, *MNRAS*, 262, 545
- Lamers, H. J. G. L. M., Zickgraf, F.-J., de Winter, D., Houziaux, L., & Zorec, J. 1998, *A&A*, 340, 117
- Larsen, S. S. 2004, *A&A*, 416, 537
- Lau, R. M., Heida, M., Kasliwal, M. M., & Walton, D. J. 2017, *ApJ*, 838, L17
- Lau, R. M., Kasliwal, M. M., Bond, H. E., et al. 2016, *ApJ*, 830, 142
- Lee, M. G. 1996, *AJ*, 112, 1438
- Liu, J. 2011, *ApJS*, 192, 10
- Long, K. S., Kuntz, K. D., Blair, W. P., et al. 2014, *ApJS*, 212, 21
- Lutovinov, A. A., Revnivtsev, M. G., Tsygankov, S. S., & Krivonos, R. A. 2013, *MNRAS*, 431, 327
- MacLeod, M., Antoni, A., Murguía-Berthier, A., Macías, P., & Ramírez-Ruiz, E. 2017, *ApJ*, 838, 56
- Marks, M., Kroupa, P., Dabringhausen, J., & Pawłowski, M. S. 2012, *MNRAS*, 422, 2246
- Martínez-Núñez, S., Kretschmar, P., Bozzo, E., et al. 2017, *Space Sci. Rev.*, 212, 59
- Mineo, S., Gilfanov, M., & Sunyaev, R. 2011, *Astronomische Nachrichten*, 332, 349
- Mineo, S., Gilfanov, M., & Sunyaev, R. 2012, *MNRAS*, 419, 2095
- Misiriotis, A., Xilouris, E. M., Papamastorakis, J., Boumis, P., & Goudis, C. D. 2006, *A&A*, 459, 113
- Murray, N. & Rahman, M. 2010, *ApJ*, 709, 424
- Oskinova, L. M., Feldmeier, A., & Kretschmar, P. 2012, *MNRAS*, 421, 2820
- Paczynski, B. 1971, *ARA&A*, 9, 183
- Paczynski, B. 1976, in *IAU Symposium*, Vol. 73, *Structure and Evolution of Close Binary Systems*, ed. P. Eggleton, S. Mitton, & J. Whelan, 75
- Page, M. J., Brindle, C., Talavera, A., et al. 2012, *MNRAS*, 426, 903
- Postnov, K. A. & Yungelson, L. R. 2014, *Living Reviews in Relativity*, 17, 3
- Ramachandran, V., Hamann, W.-R., Hainich, R., et al. 2018, *ArXiv e-prints* [[arXiv:1802.07494](https://arxiv.org/abs/1802.07494)]
- Repetto, S., Davies, M. B., & Sigurdsson, S. 2012, *MNRAS*, 425, 2799
- Robitaille, T. P. & Whitney, B. A. 2010, *ApJ*, 710, L11
- Sander, A. A. C., Fürst, F., Kretschmar, P., et al. 2017, *ArXiv e-prints* [[arXiv:1708.02947](https://arxiv.org/abs/1708.02947)]
- Schneider, F. R. N., Sana, H., Evans, C. J., et al. 2018, *Science*, 359, 69
- Servillat, M., Coleiro, A., Chaty, S., Rahoui, F., & Zurita Heras, J. A. 2014, *ApJ*, 797, 114
- Shenar, T., Hainich, R., Todt, H., et al. 2016, *A&A*, 591, A22
- Smith, L. F., Biermann, P., & Mezger, P. G. 1978, *A&A*, 66, 65
- Terman, J. L., Taam, R. E., & Hernquist, L. 1995, *ApJ*, 445, 367
- Thorne, K. S. & Zytow, A. N. 1975, *ApJ*, 199, L19
- Tutukov, A. & Yungelson, L. 1973, *Nauchnye Informatsii*, 27, 70
- van den Heuvel, E. P. J. & De Loore, C. 1973, *A&A*, 25, 387
- Vanbeveren, D., De Loore, C., & Van Rensbergen, W. 1998, *A&A Rev.*, 9, 63
- Walter, R., Lutovinov, A. A., Bozzo, E., & Tsygankov, S. S. 2015, *A&A Rev.*, 23, 2
- Wang, S., Liu, J., Qiu, Y., et al. 2016, *ApJS*, 224, 40
- Webbink, R. F. 1984, *ApJ*, 277, 355
- Weidner, C. & Kroupa, P. 2006, *MNRAS*, 365, 1333
- Woosley, S. E., Heger, A., & Weaver, T. A. 2002, *Reviews of Modern Physics*, 74, 1015
- Wysocki, D., Gerosa, D., O’Shaughnessy, R., et al. 2018, *Phys. Rev. D*, 97, 043014

Appendix A: Notes on some interesting individual objects

SPIRITS 16ajc in the galaxy M 83 is extensively discussed by Kasliwal et al. (2017). The source went into IR-outburst in 2010. No optical or near-IR counterpart was detected in ground-based follow-up in 2014, but shock-excited H_2 emission lines were seen in the spectrum measured on the 2014 June 8 spectrum. Our search for X-ray sources associated with IR-transients revealed that the X-ray source [LKB2014] X100 in the “M 83 Chandra X-Ray Point Source Catalog” (Long et al. 2014) is $0''.5$ apart from the coordinates of SPIRITS 16ajc. [LKB2014] X100 has an X-ray luminosity of $L_X = 8.5 \times 10^{35} \text{ erg s}^{-1}$ and is identified in the catalog as a supernova remnant (SNR) candidate. This identification is based on the previous detection of an SNR candidate [BWL2012] 063 at this location in the optical (Blair et al. 2012). The optical observations were obtained on 2009 April 26 and 27, i.e., pre-IR outburst. Kasliwal et al. (2017) inspected the HST WFC3 images of the area around SPIRITS 14ajc taken in 2012 (i.e., during the IR outburst) They noted a faint emission nebula close to 14ajc in $H\alpha + [N II]$ filter image, but commented that this nebula is outside of the 14ajc position error circle. It is possible that this faint emission nebula is the SNR candidate, and thus is not associated with 14ajc.

The galaxy NGC 1313 is a host of a few SPIRITS transients. SPIRITS 16tj was detected in this galaxy on 2016-08-05 (Jencson et al. 2017). Although the galaxy was observed by both the *Chandra* and *XMM-Newton* telescopes, no X-ray source potentially associated with 16tj was found in the X-ray catalogs. An optical source likely associated with SPIRITS 16tj was detected by the *XMM-Newton* optical/UV telescope (OM) (Page et al. 2012). The catalog position of the OM UV source is $0''.18$ source from 16tj, while its statistical positional uncertainty is $0''.62$. The $B_{\text{Vega}} = 22.6 \pm 0.4 \text{ mag}$. The source is associated with the star cluster [L2004] 1313-464 with $V=19.9 \text{ mag}$ (Larsen 2004). The optical and UV source is seen off-set by $\sim 0''.2$ from nominal coordinates of the 16tj in the pre-outburst HST images obtained on 2014-02-19. A comparison of pre- and post-outburst HST can help to establish whether 16tj was indeed associated with an optical star in a cluster. Optical/UV sources are also seen in the vicinity of the SPIRITS 16tg and SPIRITS 16tf events. On the other hand, no optical precursor to SPIRITS 16th is obvious in the pre-outburst HST images.

SPIRITS 15aht discovered on 2016-1-14 (Jencson et al. 2016) is likely associated with the nova candidate PNV J09551857+6904223. The latter has $H\alpha$ magnitude $19.5 \pm 0.1 \text{ mag}$ and was discovered on 2015 Oct. 14.198 UT (Hornoch et al. 2015). This nova is only $0''.5$ away from 15aht. These two events are very probably associated.

SPIRITS 15ael in the dwarf elliptical galaxy NGC 205 was detected only $0''.6$ away from the UV source XMMOM J004022.8+414136 (positional error $0''.53$). *XMM-Newton* observations were carried out on 2004-01-02, i.e., more than a decade prior to the detection of an IR transient. Likely, the IR transient and the UV source are associated with the objects cataloged by Lee (1996). Unfortunately, the archival *XMM-Newton* and *Chandra* observations are quite shallow.

SPIRITS 15ud in the galaxy M 100 is probably associated with the $H II$ region [K98d] 988, while SPIRITS 14bsb is associated with the $H II$ region [SCM2003] NGC 625 5 in the galaxy NGC 625.

SPIRITS 16az in the galaxy NGC 4490 was in the field of view of six *XMM-Newton* observations in 2002, 2008, and 2015. In none of these observations was NGC 4490 X40 detected as

a point source. The reason may be that the object was not outbursting during the *XMM-Newton* observations, or because it is located in a crowded area filled with diffuse X-rays and thus is difficult to detect with *XMM-Newton*.

SPIRITS 14axa has peaked at 2014-06-13 (Kasliwal et al. 2017). This transient is only $0''.44$ away from a nova discovered on 2014 May 21.92 (Hornoch & Kucakova 2014). These two events are likely related.

SPIRITS 17mj in M 81 is only $1''.4$ away from the X-ray source NGC 3031-X165 listed in the Liu (2011) catalog of X-ray sources in nearby galaxies. However, no counterparts are found in other X-ray catalogs. The visual inspection of *Chandra* X-ray images does not reveal an obvious X-ray source at this position (in many observations, the source lies in the CCD gap).

Table A.1. Infrared transients, SPIRITS, considered in this work. *Chandra* exposure times shown in col. 6 are approximate and can be used only for a rough guidance

| | RA | DEC | SPIRITS | Host galaxy | CXO exposure time [ks] | comments |
|----|-------------|-------------|---------|---------------|---------------------------|---|
| 1 | 01:35:01.12 | -41:26:07.2 | 17eq | NGC0625 | 60 | |
| 2 | 13:25:17.57 | -42:59:21.0 | 17bf | Cen A | 1100 | |
| 3 | 03:46:35.25 | +68:01:57.1 | 17c | IC 342 | 70 | |
| 4 | 03:18:21.22 | -66:29:51.1 | 16tj | NGC 1313 | 70 | optical/UV src at 0'2 <i>XMM-Newton</i> OM & HST, cluster [L2004] n1313-464 |
| 5 | 03:18:27.20 | -66:28:38.6 | 16th | NGC 1313 | 85 | |
| 6 | 03:18:16.92 | -66:28:57.7 | 16tg | NGC 1313 | 85 | UV src at 0'5 in the HST image |
| 7 | 03:18:04.82 | -66:30:17.8 | 16tf | NGC 1313 | 85 | UV src at 0'5 in the HST image |
| 8 | 13:05:43.63 | -49:27:04.2 | 16rz | NGC 4945 | 450 | |
| 9 | 13:05:07.36 | -49:32:40.0 | 16rs | NGC 4945 | 126 | |
| 10 | 13:05:22.33 | -49:28:31.2 | 16rp | NGC 4945 | 450 | |
| 11 | 13:05:19.00 | -49:28:50.8 | 16rn | NGC 4945 | 450 | |
| 12 | 13:36:47.15 | -29:52:58.6 | 16pr | M 83 | 840 | |
| 13 | 13:37:01.50 | -29:54:26.8 | 16po | M 83 | 840 | |
| 14 | 03:46:27.63 | +68:13:42.0 | 16ph | IC 342 | 70 | |
| 15 | 13:36:40.73 | -29:52:41.7 | 16oz | M 83 | 840 | |
| 16 | 13:18:53.54 | -21:04:14.5 | 16oj | NGC 5068 | 54 | |
| 17 | 14:02:57.80 | +54:22:50.6 | 16kp | M 101 | 800 | |
| 18 | 12:50:50.53 | +41:06:04.4 | 16ko | M 94 | 74 | |
| 19 | 12:40:06.02 | -11:38:14.1 | 17as | M 104 | 92 | 1'8 away from the globular cluster [LFB2001] C-101 |
| 20 | 13:05:36.89 | -49:23:38.2 | 17ar | NGC 4945 | 90 | |
| 21 | 03:47:29.89 | +68:03:13.1 | 17g | IC 342 | 14 | |
| 22 | 00:40:20.95 | +41:39:35.6 | 16abq | M 110 | 9 | |
| 23 | 03:46:49.27 | +68:03:52.9 | 17lk | IC 342 | 72 | |
| 24 | 03:46:03.55 | +68:08:48.2 | 17lg | IC 342 | 72 | |
| 25 | 03:46:07.32 | +68:07:59.0 | 17lc | IC 342 | 72 | |
| 26 | 06:16:27.78 | -21:22:51.7 | 17lb | IC 2163 | 62 | |
| 27 | 13:25:33.08 | -43:00:51.6 | 17kw | Cen A | 1100 | |
| 28 | 13:25:32.03 | -43:00:41.3 | 17kq | Cen A | 1100 | |
| 29 | 13:25:20.3 | -42:59:20.2 | 17kp | Cen A | 1100 | |
| 30 | 13:36:57.42 | -29:50:19.1 | 17kj | M83 | 810 | |
| 31 | 13:25:22.18 | -43:01:17.5 | 17kf | Cen A | 1100 | |
| 32 | 13:25:29.44 | -43:01:40.0 | 17kc | Cen A | 1100 | |
| 33 | 13:37:16.22 | -29:54:18.7 | 17ka | M83 | 810 | |
| 34 | 12:18:50.33 | +47:18:11.5 | 17fo | NGC4258 | 500 | |
| 35 | 14:03:01.29 | +54:22:54.4 | 17fm | M101 | 885 | |
| 36 | 23:57:44.77 | -32:34:58.4 | 17fe | NGC 7793 | 190 | |
| 37 | 09:55:18.54 | +69:04:22.8 | 15aht | M81 | 800 | 0'5 offset from a nova candidate 2015 Oct. 14.198 UT |
| 38 | 07:36:37.40 | +65:38:02.6 | 15ahg | NGC 2403 | 80 | |
| 39 | 03:46:17.57 | +68:08:44.7 | 15agl | IC342 | 30 | |
| 40 | 20:34:59.65 | +60:11:18.1 | 15afp | NGC6946 | 163 | |
| 41 | 02:22:40.29 | +42:23:53.5 | 15aev | NGC 891 | 110 | |
| 42 | 00:40:22.82 | +41:41:36.4 | 15ael | NGC 205 | 9 | optical source 0'6 V=20.6 mag |
| 43 | 15:22:05.55 | +05:03:15.9 | 15ade | NGC 5921 | not observed | |
| 44 | 03:18:23.63 | -66:30:24.2 | 15aag | NGC1313 | 65 | |
| 45 | 13:36:57.08 | -29:53:13.3 | 15aac | M83 | 810 | |
| 46 | 13:34:44.21 | -45:32:25.5 | 15yq | ESO270G017 | not observed | |
| 47 | 00:54:48.74 | -37:43:13.7 | 15yf | NGC300 | 200 | |
| 48 | 12:34:19.00 | +06:28:15.7 | 15ue | NGC 4532 | not observed | |
| 49 | 12:22:55.29 | +15:49:22.0 | 15ud | NGC 4321 | 134 | H II region |
| 50 | 11:18:19.10 | -32:51:06.9 | 15ua | NGC 3621 | not observed | |
| 51 | 01:35:06.72 | -41:26:13.4 | 14bsb | NGC 625 | 60 | H II region |
| 52 | 00:54:49.68 | -37:39:51.2 | 14bmc | NGC300 | 150 | |
| 53 | 22:02:41.52 | -51:17:34.5 | 14beq | IC5152 | not observed | no optical counterpart in post-outburst images |
| 54 | 12:56:43.25 | +21:42:25.7 | 14bay | NGC 4826 | 27 | |
| 55 | 12:29:03.16 | +13:11:30.7 | 16ix | NGC 4458 | 34 | |
| 56 | 12:56:39.10 | +21:41:43.2 | 16fz | NGC 4826 | 27 | |
| 57 | 12:15:38.61 | +36:19:46.9 | 16ea | NGC 4214 | 56 | |
| 58 | 12:30:27.78 | +41:39:41.3 | 16az | NGC 4485/4490 | 78 | optical 0'6, X-ray at 1'4, HMXB? |
| 59 | 09:32:11.64 | +21:30:03.0 | 16aj | NGC 2903 | 93 | |
| 60 | 03:18:09.34 | -66:29:59.4 | 15qv | NGC1313 | 90 | |
| 61 | 03:18:15.26 | -66:30:03.4 | 15qo | NGC1313 | 85 | |
| 62 | 22:02:42.07 | -51:17:22.3 | 15qh | IC 5152 | not observed | |
| 63 | 10:44:02.36 | +11:42:15.1 | 15pz | NGC 3351 | 128 | |
| 64 | 13:37:08.37 | -29:50:19.7 | 15nz | M83 | 840 | |
| 65 | 12:39:54.87 | +61:36:46.3 | 15mr | NGC 4605 | not observed | |
| 66 | 14:03:10.76 | +54:22:49.1 | 15mo | M101 | 850 | |
| 67 | 14:03:49.44 | +54:20:50.7 | 15mn | M101 | 680 | |
| 68 | 10:03:18.90 | +68:43:52.1 | 15mk | NGC 3077 | 60 | |
| 69 | 09:55:28.72 | +69:39:58.6 | 14qk | M82 | 813 | |
| 70 | 12:50:49.56 | +41:05:52.7 | 14afv | NGC4736 | 71 | |
| 71 | 13:05:30.87 | -49:26:50.8 | 14agd | NGC 4945 | 449 | |
| 72 | 13:36:52.95 | -29:52:16.1 | 14ajc | M83 | 840 | X-ray source at 0'5, SNR? |
| 73 | 13:37:05.02 | -29:48:56.2 | 14ajd | M83 | 840 | |
| 74 | 14:02:55.51 | +54:23:18.5 | 14aje | M101 | 885 | |
| 75 | 13:37:12.71 | -29:49:14.9 | 14ajp | M83 | 508 | |
| 76 | 13:36:54.81 | -29:52:33.7 | 14ajr | M83 | 840 | |
| 77 | 03:47:03.17 | +68:09:05.3 | 14ave | IC342 | 15 | |
| 78 | 09:56:01.52 | +69:03:12.5 | 14axa | M81 | 790 | associated with nova PNV J09560160+6903126 |
| 79 | 07:36:34.70 | +65:39:22.4 | 14axb | NGC2403 | 38 | |
| 80 | 13:39:50.99 | -31:38:46.0 | 14bay | NGC5253 | 191 | |
| 81 | 12:56:47.90 | +21:41:13.4 | 17pe | M64 | 28 | |
| 82 | 13:18:51.52 | -21:01:35.1 | 17nx | NGC 5068 | 54 | |
| 83 | 09:55:36.20 | +69:06:21.0 | 17mj | M81 | 300 | possible X-ray source at 1'4 |
| 84 | 07:36:35.94 | +65:37:26.5 | 17mi | NGC 2403 | 230 | |
| 85 | 13:05:11.16 | -49:30:19.0 | 17mb | NGC 4945 | 300 | |

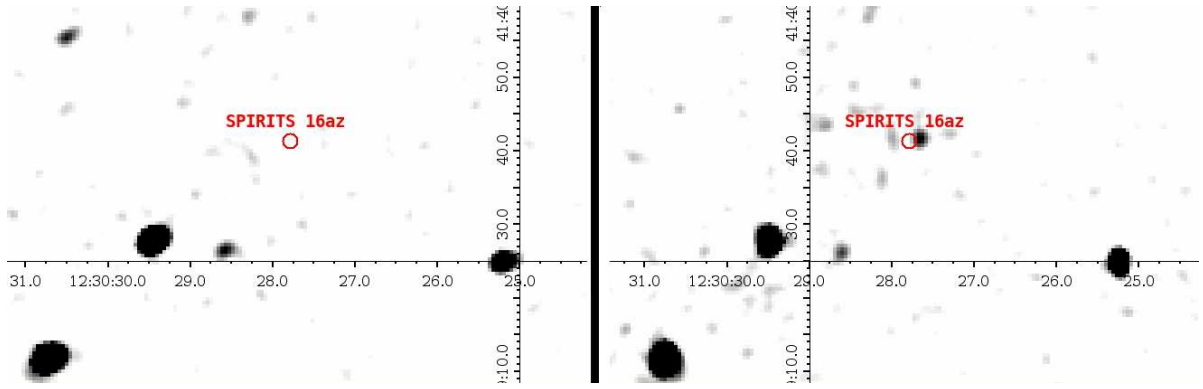


Fig. A.1. Archival not-binned broad-band (0.2–12 keV) X-ray images of NGC 4490 around the position of SPIRITS 16az as indicated by the red circles in each panel. The circle radii are $1''$. The images were obtained by the *Chandra* ACIS-S camera on 2004-07-29 with an exposure time ~ 39 ks (left panel) and on 2000-11-03 with an exposure time ~ 40 ks (right panel). The X-ray images are shown on linear scale and were smoothed to facilitate perception of the source. North is up, east is to the left.